

Self-motion behaviors of kinematically redundant manipulator for continuous path planning

Setyamartana Parman¹, Mahmud Iwan Solihin²

¹*Fakulti Teknologi Kejuruteraan Mekanikal dan Pembuatan, Universiti Teknikal Malaysia Melaka, 75450 Ayer Keroh, Melaka, Malaysia*

²*Faculty of Engineering, Technology and Built Environment, UCSI University, Kuala Lumpur 56000, Malaysia*

Abstract—This paper presents self-motion behaviors of 3-DOF planar robotic arm when it tracks a predefined end-effector path. In this case, the self-motion contributes to geometry of a motion envelope. The Bezier curve degree fifth is utilized as the tracked path. Different geometry of the motion envelope can be used to avoid collision while it also follows the tracked path accurately. A theta global as closed form solution of 3-DOF planar robot is modeled as a polynomial degree sixth. A Genetic Algorithm (GA) as one of meta-heuristic optimizations is used to find optimal solution of the path planning approach. An effect of initial and final joint angles in the robotic arm motion is also investigated. The theta global trajectories are also possible to contain an imaginary number. The imaginary number of the theta global trajectories can be used as a sign that position errors are present and the trajectories need to be repaired using the self-motion analysis.

Keywords—Self-motion, genetic algorithm, path planning, redundant manipulator.

I. INTRODUCTION

An arm robot is very fascinating tool to be utilized to accomplish a job which contains manipulation. The method to generate trajectories that exhibit zero error is the main goal of the continuous path planning. Especially for kinematically redundant robot, there are many joint angle trajectories available for one instantaneous point so that the redundant manipulator has the self-motion capability. The self-motion has benefits in avoiding collision, achieving n -connectivity as well as avoiding singularity [1].

Tracking the predefined path is the problem of constructing the connected trajectories from the initial point to the final point with the end-effector path as the constraint. Regarding the existence of many available solutions for one instantaneous point, constructing the connected trajectories is non-trivial problem.

Self-motion manifold in robotics firstly introduces and investigates by [3]. Since then, the self-motion become one of the most interesting research topics in the robotic arm. Numerous papers in the self-motion have been presented [1-8]. Machmudah et al [9] proposed an interval analysis of the self-motion to generate the joint angle trajectories and employed meta-heuristic optimizations to find the optimal solution. Lin et al [10] proposed the path planning algorithm which consisted of the Swinging Search and the Crawling Control. In Swinging Search part, a collision-free configuration was computed by applying reinforcement learning to self-motion. The self-motion takes global solution of IK rather than local solution [2]. Thus, the self-motion cannot be separated from the IK problem. For tracking the curve, the IK solution is the most important thing to be considered since it is necessary to achieve the end-effector configuration. there are many research papers have been published to propose the IK solution analytically as well as numerically [11-15].

Different with previous researches where they focused mostly on the self-motion behavior for one instantaneous end-effector configuration, this research investigates the self-motion behavior when the redundant manipulator tracks the entire tracked curve. The tracked path can be considered as the trajectories composed from set of fixed end-effector configurations. For redundant robot, there are infinite Inverse Kinematics (IK) solutions available for one end-effector configuration [2]. Thus, the motion analysis of the redundant robot can be very complex. The problem become how to choose the trajectories among many possible solutions.

This paper models the problem of the continuous motion of the redundant 3-DOF planar series manipulator by considering the theta global trajectories as polynomial function. For 3-DOF planar robot, the theta global variable, which is the summation of the first, second, and third joint angles, contributes to the self-motion of one instantaneous point. When the theta global is modeled as the continuous function, the global behavior of the arm robot motion can be visualized more clearly by the motion

Corresponding Author:

Setyamartana Parman
Fakulti Teknologi Kejuruteraan Mekanikal dan Pembuatan, Universiti Teknikal Malaysia Melaka, 75450 Ayer Keroh, Melaka, Malaysia

setyamartana@utem.edu.my

envelope constructed during tracking the entire path. Different theta global for one end-effector position represents different point in the self-motion manifold. For continuous path planning, the trajectory generator needs to create the trajectories that are connected while it also tracks the path. Using polynomial function as the theta global trajectories, the joint angle trajectories will be guaranteed connected following the polynomial function. The envelope of motion is used to visualize these behaviors.

II. SELF-MOTION TO REPAIR UNFEASIBLE TRAJECTORIES

The self-motion capability of kinematically redundant manipulator is one of the most interesting behaviors of the arm robot where it can be used to repair the unfeasible trajectories. The self-motion has a benefit in repairing the unfeasible trajectories regarding the collision, the singularity, as well as the connectivity. The self-motion is the case when the position of the end-effector is fixed and the positions of the joint angles are moved. For 3-DOF planar robot, different value of the theta global for the same end-effector position represents the self-motion contribution in the manipulator motion. Different theta global trajectories means that the postures changes or motion envelope is also different. Instead of analyzing the self-motion for just one instantaneous point, this paper considers the self-motion when the manipulator tracks the entire tracked curve. Since the end-effector path does not change, all different trajectories are due to the contribution of the self-motion.

For the redundant manipulator, there are many possible configurations for one instantaneous end-effector position. When the obstacle is present, besides the collision-free requirement, the chosen trajectories should have n -connectivity and smoothness. Figure 1a illustrates the example of the wrong trajectories which correlate with the wrong postures, Fig. 1b, of the link configurations. During the motion, the posture of the link configuration is changed. Kinematically redundant manipulator has capability of the self-motion that give the advantage in avoiding collision and finding the correct posture; however, since there are many possible configurations for one end-effector position, finding the feasible trajectories is non-trivial problem. The posture in Fig. 1b is possible to be reconstructed because the redundant manipulator has the self-motion capability. Figure 2 is the example of the feasible motion where the joint angle trajectories. Figure 2b is very smooth joint angle trajectories and the postures of manipulator, as shown in Fig 2b, are also proportional.

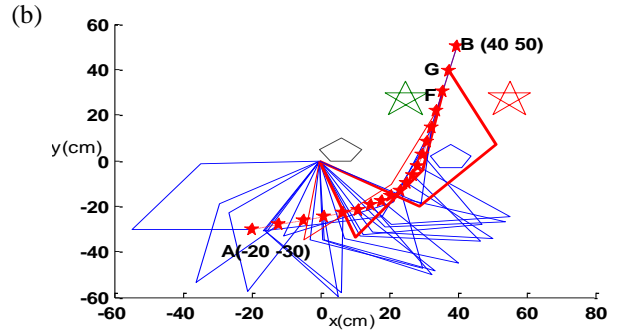


Figure 1. (a). Joint angle trajectories (b). wrong posture of (a)

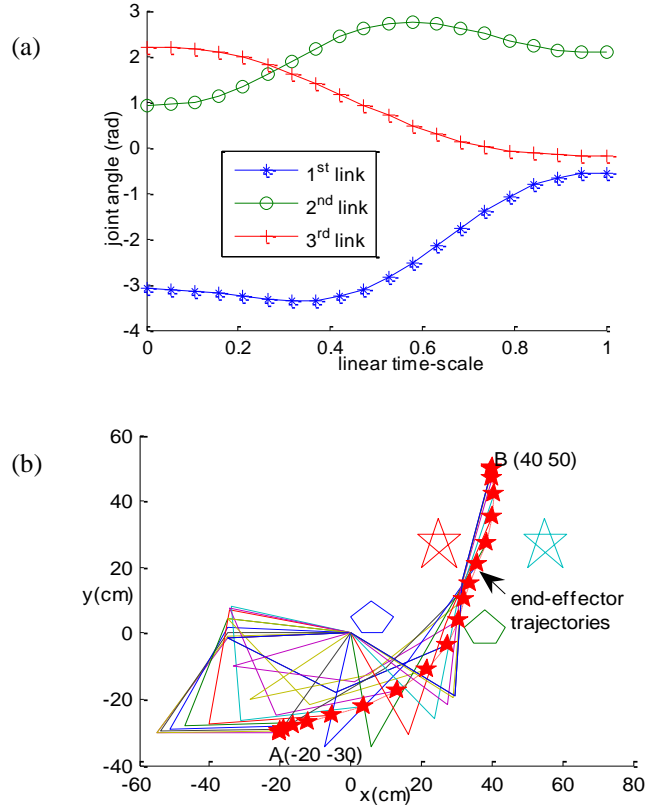


Figure 2. Repair trajectories by self-motion (a) Joint angle trajectories (b). proper posture of (a)

III. MODIFICATION OF IK SOLUTION OF 3-DOF PLANAR ROBOT: THETA GLOBAL AS POLYNOMIAL FUNCTION

3-DOF planar robot has the closed form solution using algebra method [16]. There is the variable utilized, namely the theta global.

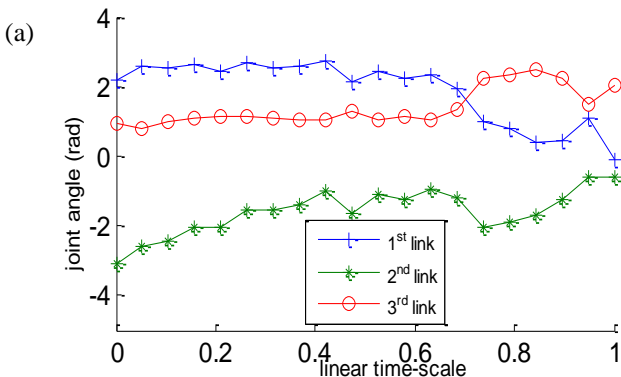
$$\theta_g = -\theta_1 - \theta_2 + \theta_3 \quad (1)$$

$$w_x = P_x - l_1 \cos \theta_g ; w_y = P_y - l_1 \sin \theta_g \quad (2)$$

where $P_x, P_y, \theta_g, \theta_1, \theta_2,$ and θ_3 are the position of end-effector in Cartesian coordinate, the theta global, the first, second, and third joint angles, respectively.

The cosine and sine of second joint angle can be obtained by the following

$$C_2 = \frac{(w_x^2 + w_y^2 - l_1^2 - l_2^2)}{2l_1 l_2} \quad (3)$$



$$s_2 = \pm\sqrt{1 - c_2^2} \quad (4)$$

The second joint angle can be determined by inverse tangent as follow

$$\theta_2 = a \tan 2 (s_{21}, c_{21}) \quad (5)$$

The first joint angle can be obtained as follows

$$\Delta = w_x^2 + w_y^2 \quad (6)$$

$$s_1 = \frac{(l_1 + l_2 c_2)w_y - (l_2 s_2 w_x)}{\Delta} \quad (8)$$

$$c_1 = \frac{(l_1 + l_2 c_2)w_x + (l_2 s_2 w_y)}{\Delta} \quad (9)$$

$$\theta_1 = a \tan 2 (s_1, c_1) \quad (10)$$

where s_1 and c_1 are the sine and cosine of first joint angle, respectively.

Finally, the third joint angle can be calculated from the relation of the theta global, the first joint angle, and the second joint angle as follows

$$\theta_3 = \theta_g - \theta_1 - \theta_2 \quad (11)$$

A. Theta Global as Polynomial function

To perform the manipulation, the arm robot needs to move from the initial configuration to the final configuration. The continuous path where the end-effector should track the specific path needs to solve the inverse kinematic to construct the joint angle trajectories. 3-DOF planar robot is redundant robot which kinematically there will be many possible solutions for of one instantaneous end-effector position. For the whole motion, the joint angle trajectories should be feasible. In case of obstacle environment, besides tracking the path, it also needs to avoid collision as well as have n-connectivity.

This research will investigate the characteristic of the joint angle trajectories when the theta global as the closed form solution of 3-DOF planar robot is modeled as the continuous function of polynomial degree sixth.

The joint angle as function of time can be expressed as composition function of joint angle profile and linear time-scale as follows

$$\theta_g(t) = \theta_g(r) \circ r(t) \quad (12)$$

$$r(t) = \frac{t}{T} \quad (13)$$

where $\theta_g(t)$, $\theta_g(r)$, $r(t)$, t , and T are the theta global function of time, the global profile, linear time-scale, the time, and the total travelling time, respectively.

Using polynomial function degree sixth as theta global trajectories, the theta global profile can be expressed in the following

$$\theta_g(r) = a_{6g}r^6 + a_{5g}r^5 + a_{4g}r^4 + a_{3g}r^3 + a_{2g}r^2 + a_{1g}r + a_{0g} \quad (14)$$

where r is linear time-scale and a_{ng} is the n^{th} polynomial coefficient of theta global.

Utilizing the chain rule, the velocity and acceleration can be derived from (3) as follows

$$\dot{\theta}(t) = \dot{\theta}(r) \frac{1}{T} \quad (15)$$

$$\ddot{\theta}(t) = \ddot{\theta}(r) \frac{1}{T^2} \quad (16)$$

This research uses the boundary condition that the initial/ final velocities of the theta global and the initial/ final accelerations of the theta global are zero.

Considering all boundary conditions into Eqs. (3, 4, 5), the following equations are obtained

$$a_{0g} = \theta_{ig} ; a_{1g} = a_{2g} = 0;$$

$$a_{5g} = -3a_{6g} - 6\theta_{ig} + 6\theta_{fg} \quad (17)$$

$$a_{4g} = 0.5(-9a_{6g} - 5a_{5g}) \quad (18)$$

$$a_{3g} = \theta_{fg} - \theta_{ig} - a_{6g} - a_{5g} - a_{4g} \quad (19)$$

where a_{ng} , θ_{ng} , θ_{ig} and θ_{fg} are n th coefficient of theta global, theta global trajectories for n th link, and initial theta global and final theta global, respectively.

The theta global equation in (14) is reduced in the following:

$$\theta_g = a_{6g}r^6 + a_{5g}r^5 + a_{4g}r^4 + a_{3g}r^3 + a_{0g} \quad (20)$$

There is one unknown variable in this case, the sixth polynomial joint angle coefficient, a_{6g} .

B. General Pattern of sixth polynomial joint angle trajectories

This paper model the theta global trajectories as the polynomial degree sixth. It is very essential to obtain the pattern of the sixth-degree polynomial trajectories that creates a motion collaboration among the links during the manipulator motion.

The pattern of the joint angle trajectories can be predicted from the first and second derivatives of the joint angle polynomial function. Mathematically, they determine the location of the turning point as well as the local maximum/minimum point.

From the boundary conditions, the velocity at initial point, $r = 0$, and final point, $r = 1$, that are equal to zero mean that 0 and 1 are the roots of the first derivative of joint angle path, θ as follows

$$\frac{d\theta}{dr} = 0 \quad (21)$$

$$6a_{6g}r^5 + 5a_{5g}r^4 + 4a_{4g}r^3 + 3a_{3g}r^2 = 0$$

$$(r - 1)(r - 0)(r - r_a)(r - r_b)(r - r_c) = 0 \quad (22)$$

Other three roots, r_a , r_b , r_c can be determined from:

$$(r - 1)(r - 0) \left(\frac{6a_{6g}r^5 + 5a_{5g}r^4 + 4a_{4g}r^3 + 3a_{3g}r^2}{(r - 1)(r - 0)} \right) = 0 \quad (23)$$

From (22) and (23), the following can be obtained:

$$(r - r_a)(r - r_b)(r - r_c) = \left(\frac{6a_{6g}r^5 + 5a_{5g}r^4 + 4a_{4g}r^3 + 3a_{3g}r^2}{(r - 1)(r - 0)} \right) \quad (24)$$

This three roots, r_a, r_b, r_c , will be the roots of cubic equation. It has three possible values; three real numbers, multiple roots, or one real number and two complex numbers.

In this case, since 0 and 1 are the roots of the velocity equation, so there is possibility that these number are the part of the other three roots. Firstly, this paper will investigate this possibility. Considering 0 and 1 as the twin roots, (23) can be expressed as follows:

$$(r-1)(r-0)(r-1)(r-0) \left(\frac{6a_{6g}r^5 + 5a_{5g}r^4 + 4a_{4g}r^3 + 3a_{3g}r^2}{(r-1)^2(r-0)^2} \right) = 0$$

Solving the equation of the last root:

$$\left(\frac{6a_{6g}r^5 + 5a_{5g}r^4 + 4a_{4g}r^3 + 3a_{3g}r^2}{(r-1)^2(r-0)^2} \right) = \left(6a_{6g}r + (5a_{5g} + 12a_{6g}) \right) + \frac{r^3(4a_{4g} + 18a_{6g} + 10a_{5g}) + r^2(3a_{3g} - 5a_{5g} - 12a_{6g})}{r^4 - 2r^3 + r^2} \quad (25)$$

There are residue parts. Return back to Eqs (15, 16), for final boundary conditions, at $r=1$, the velocity and acceleration are zero, the equations are as follows:

$$\dot{\theta}(1) = 6a_{6g} + 5a_{5g} + 4a_{4g} + 3a_{3g} = 0 \quad (26)$$

$$\ddot{\theta}(1) = 30a_{6g} + 20a_{5g} + 12a_{4g} + 6a_{3g} = 0 \quad (27)$$

Eliminate Eqs (26, 27) in the following:

$$(27) \rightarrow 30a_{6g} + 20a_{5g} + 12a_{4g} + 6a_{3g} = 0$$

$$(26) \times 2 \rightarrow \frac{12a_{6g} + 10a_{5g} + 8a_{4g} + 6a_{3g} = 0}{18a_{6g} + 10a_{5g} + 4a_{4g} = 0} \quad (28)$$

$$(26) \times 3 \rightarrow 18a_{6g} + 15a_{5g} + 12a_{4g} + 9a_{3g} = 0$$

$$(27) \rightarrow \frac{30a_{6g} + 20a_{5g} + 12a_{4g} + 6a_{3g} = 0}{-12a_{6g} - 5a_{5g} - 3a_{3g} = 0} \quad (29)$$

The Equations (28, 29) are the coefficient of r^3 and r^2 of the residue part of (25) that are equal to zero, so that the residual part will be equal to zero also.

Since this agrees with all equation in the sixth polynomial joint angle trajectories, thus it proves that 0 and 1 are part of the other three roots. From (25), another root is $-\frac{5}{6}a_{5g} - 2a_{6g}$.

So that, we can write (21) into the following:

$$6a_{6g}r^5 + 5a_{5g}r^4 + 4a_{4g}r^3 + 3a_{3g}r^2 = 0$$

$$(r-1)^2(r-0)^2 \left(6a_{6g}r + (5a_{5g} + 12a_{6g}) \right) = 0 \quad (30)$$

From this result, the roots of the first derivative of θ are

$$r_1 = 0 \rightarrow \text{twin roots, turning point}$$

$$r_2 = 1 \rightarrow \text{twin roots, turning point}$$

$$r_3 = -5a_{5g} - 12a_{6g} \rightarrow \text{turning point}$$

These roots give the information of the turning point and the local maximum/minimum point. For $0 \leq r \leq 1$, these three roots are three possible locations of optimum points. The exact local optimum position depends on the value of a_{6g} . For example, if $\theta(r_1) \geq \theta(r_2) \geq \theta(r_3)$, then $\theta(r_1)$ is the maximum point and $\theta(r_3)$ is the minimum point.

The location of the third optimum point depends on the a_{6g} . Assume that there is no restriction of a_{6g} value, for a_{6g} approaching infinity the value of this optimum point is as follows

$$\lim_{a_{6g} \rightarrow \infty} (6a_6r + (5a_5 + 12a_6)) = 0.5 \quad (31)$$

The acceleration conditions where they are chosen to be zero at initial point and final point give the characteristic of the

inflection point of the joint angle graph. It determines the roots of the second derivative of the joint angle as follows:

$$\ddot{\theta}(r) = 30a_{6g}r^4 + 20a_{5g}r^3 + 12a_{4g}r^2 + 6a_{3g}r$$

$$= 15a_{6g}r^4 + 10a_{5g}r^3 + 6a_{4g}r^2 + 3a_{3g}r = 0 \quad (32)$$

Since the acceleration of the initial point, $r=0$, and the final point, $r=1$, are zero, it means that 0 and 1 are two of the roots of the second derivative of joint angle path, θ .

$$(r-1)(r-0) \left(\frac{15a_{6g}r^4 + 10a_{5g}r^3 + 6a_{4g}r^2 + 3a_{3g}r}{(r-1)(r-0)} \right) = 0$$

$$(r-1)(r-0) \left(15a_{6g}r^2 + r(10a_{5g} + 15a_{6g}) + (6a_{4g} + 10a_{5g} + 15a_{6g}) \right) = 0 \quad (33)$$

Thus, four possible inflection points are:

$$r_1 = 1$$

$$r_2 = 0$$

$$r_{3,4} = \frac{- (10a_{5g} + 15a_{6g}) \pm \sqrt{(10a_{5g} + 15a_{6g})^2 - 4(15a_{6g})(6a_{4g} + 10a_{5g} + 15a_{6g})}}{30a_{6g}} \quad (34)$$

The value of third and fourth inflection points depends on the value of a_{6g} . For very large a_{6g} , the location of these roots can be determined by calculating the limits when a_{6g} approaching infinity as follows

$$\lim_{a_{6g} \rightarrow \infty} \frac{- (10a_{5g} + 15a_{6g}) + \sqrt{(10a_{5g} + 15a_{6g})^2 - 4(15a_{6g})(6a_{4g} + 10a_{5g} + 15a_{6g})}}{30a_{6g}} = 0.7236$$

$$\lim_{a_{6g} \rightarrow \infty} \frac{- (10a_{5g} + 15a_{6g}) - \sqrt{(10a_{5g} + 15a_{6g})^2 - 4(15a_{6g})(6a_{4g} + 10a_{5g} + 15a_{6g})}}{30a_{6g}} = 0.2764$$

According to these results, 0 and 1 are the turning point as well as the inflection point. Following the entire characteristics of sixth degree polynomial joint angle path presented above, the pattern of the joint angle trajectories can be plotted as illustrated in Fig 3.

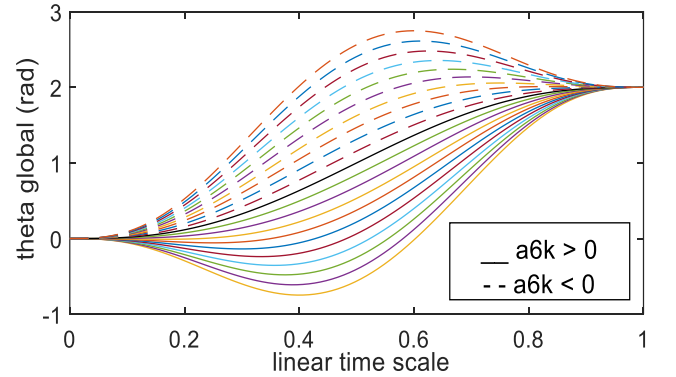


Figure 3. Polynomial degree sixth profiles of theta global

IV. GENETIC ALGORITHM

A. Objective functions

The objective function is to minimize the joint angle traveling distance of theta global while satisfying all constraints.

The joint angle traveling distance can be formulated as follows

$$f_{\theta} = \int_0^1 \sqrt{1 + \left(\frac{d\theta_g(r)}{dr} \right)^2} dr \quad (35)$$

where $\theta_g(r)$ is the theta global and r is the linear time-scale, respectively.

The interesting of this method is the root of (4). It should be noted that the imaginary number is also the possible solution of this root equation. Thus, the following constraint containing the requirement that all s_2 are real number should be considered

$$\sqrt{1 - c_2^2} \in R \quad (36)$$

For finding the theta global as continuous function at obstacle environment the constraints are the avoiding collision and (35) while for the self-motion at obstacle-free environment, the constraint is (35).

B. Genetic algorithm

This paper employs the real code GA. In the computational process, the GA is blind where it only requires to code the unknown variables and the analysis individual fitness value [17]. Other search methods require an additional information to work properly. For example, information of derivatives is necessary for a gradient technique.

There are three main operators in the GA: reproduction, crossover, and mutation. Figure 4 illustrates the GA procedure. A crossover is a process of randomly picking one or more individual as parents and swapping segments of the parents. To achieve genetic diversity from one generation of a population, the mutation procedure is implemented. The mutation changes the values of chromosomes to improve the quality of new offspring.

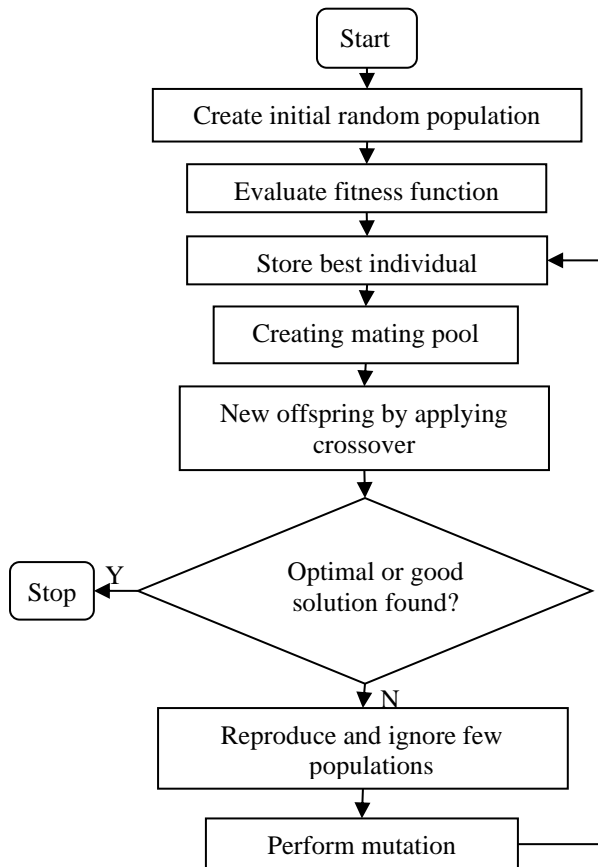


Figure 4. Genetic Algorithm

V. RESULTS AND DISCUSSIONS

A simulation in MATLAB has been done, by coding in m file. 3-DOF planar robot has the lengths 30cm, 30cm, and 20 cm for first, second, and third links, respectively. The hypermutation GA is used, with 0.4 as the mutation rate. It used 20 individuals in the population, 100 generations, and 0.5 as a selection rate. The interval of the searching area for sixth polynomial coefficient is $-200 \leq a_{6g} \leq 200$.

There are two Bezier curves degree fifth utilized as the tracked curve as illustrated in Fig 5. Detail of these tracked curves can be seen in Table 1.

Table 1. Bezier curve tracked path control points

Case	B_0	B_1	B_2	B_3	B_4	B_5
I	(40,-10)	(70,50)	(20,50)	(20,-10)	(38,54)	(60,-10)
II	(60,0)	(30,10)	(120,20)	(10,30)	(60,34)	(60,40)

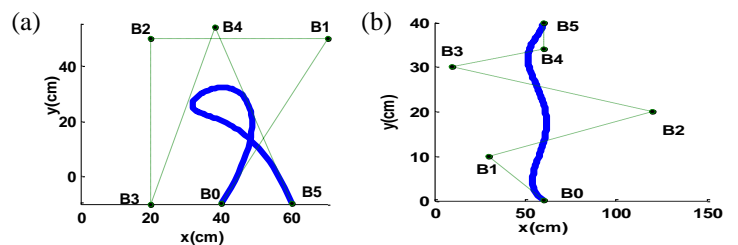


Figure 5. Fifth Bezier tracked path (a) case I (b) case II

A. Case I

First control point, B_0 , and fifth control point, B_5 , have many possible joint angle compositions to configure them regarding the self-motion capability. The initial and final joint angles are chosen as in Table 2.

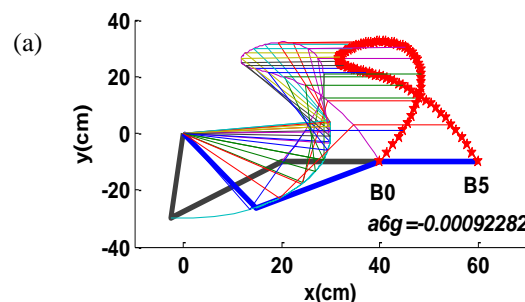
Table 2. Bezier curve tracked path control points

Case	B_0	B_1	B_2	B_3	B_4	B_5
I	40,-10)	(70,50)	(20,50)	(20,-10)	(38,54)	(60,-10)
II	60,0)	(30,10)	(120,20)	(10,30)	(60,34)	(60,40)

Table 3. Initial and final joint angles of case I

	θ_1 (rad)	θ_2 (rad)	θ_3 (rad)
initial	-1.6551	2.3765	-0.717367
final	-1.06	1.6252	-0.56002

Figure 6a shows the result of the motion envelope obtained by the GA during 100 generations. The joint angles trajectories and theta global of this result is shown in Fig. 6b. The polynomial coefficient, a_{6g} , obtained is -0.000923.



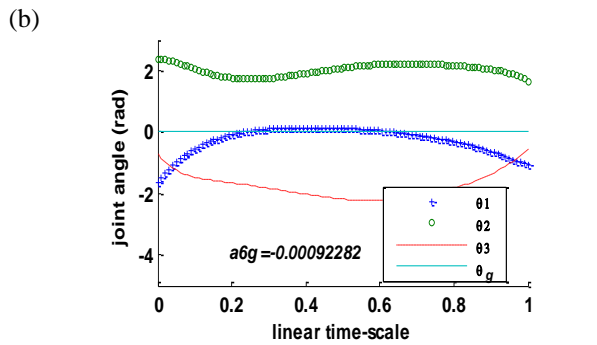


Figure 6. (a) Motion envelope (b) joint angle trajectories

A.1. Other motion envelopes to track predefined curve

The polynomial coefficient of the theta global function contributes to different motion envelope. Figures 7a and 7b show the motion envelope and the joint angle trajectories when the polynomial coefficient is 75. Figures 8a and 8b show the motion envelope and the joint angle trajectories when the polynomial coefficient is -75. From those graphs, it shows that a_{θ_g} obtained in Fig. 6 has the minimum joint angle traveling distance where the graph of theta global trajectories is minimum and the motion envelope is also very compact as compare with the graphs of $a_{\theta_g} = 75$ and $a_{\theta_g} = -75$.

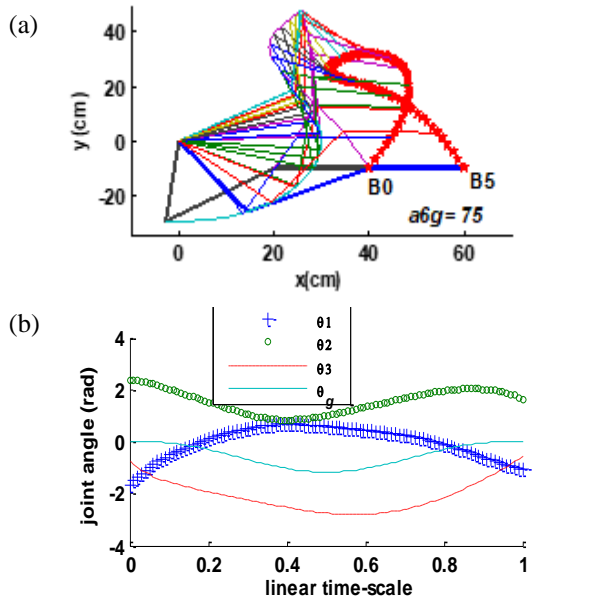


Figure 7. $a_{\theta_g} = 75$ (a) Motion envelope (b) joint angle trajectories

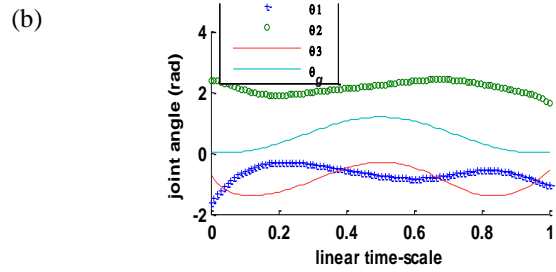
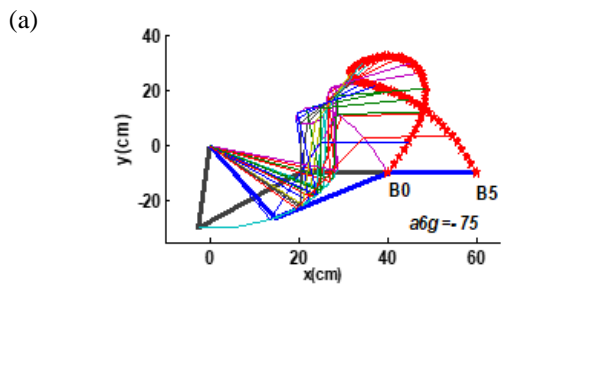


Figure 8. $a_{\theta_g} = -75$ (a) Motion envelope (b) joint angle trajectories

A.2. Collision-free continuous path planning

Previous section has shown that different polynomial coefficient of theta global contributes to the different motion envelope. This behavior is very useful in achieving the collision-free motion in the obstacle environment. Considering to place three obstacles in the environment, this section employs the hyper mutation GA to find the feasible sixth polynomial coefficient in such a way so that the robotic arm is able to track the curve while it also avoids the collision. Figure 9 shows the motion envelope obtained during 100 iterations. The polynomial coefficient resulted from this case is -97.7008.

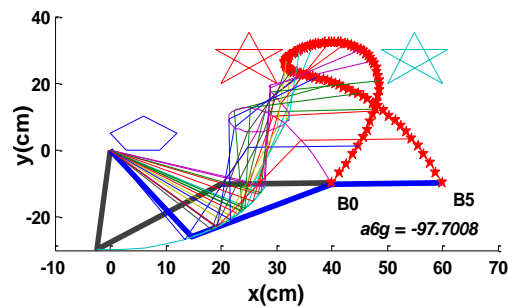
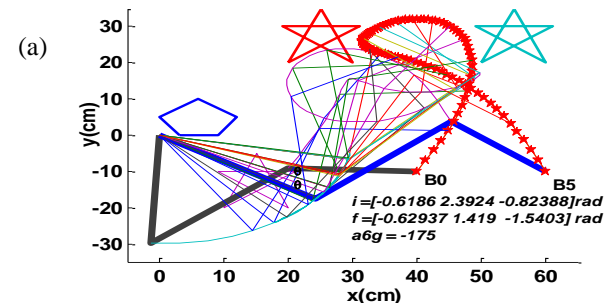


Figure 9. Collision-free motion envelope when obstacles are present

Machmudah et al [18] has been investigated that choosing the proper initial and final joint angle is very important in avoiding collision. Yao et al [3] also noticed that the bad start configuration in path planning may experience a failure in finding the feasible trajectories. In this paper, using the approach of the theta global as the continuous function, it also has been observed that when the initial and final joint angles are not proper, the collision-free path cannot be found. Figure 10a shows the example of motion envelope from the wrong initial and final configurations. These wrong configurations are $[-0.6186 \ 2.3924 \ -0.82388]$ rad for initial configuration and $[-0.62937 \ 1.419 \ -1.5403]$ rad for final configuration. Figure 10b shows the joint angle trajectories of this wrong initial and final joint angles configuration.



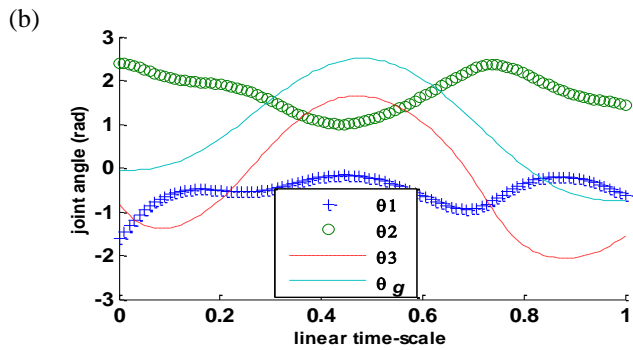


Figure 10. Example of wrong composition of the initial and final configurations. The collision-free trajectories are failure to be obtained.

B. Case II

The second Bezier curve as the tracked curve is ε -like geometry. For first simulation of the second case, the initial and final joint angles used are $[-0.84564 \ 1.6821 \ -0.82723]$ rad and $[0.43791 \ 0.69092 \ -1.1208]$, respectively. Figure 11a shows the results of the motion envelope and Fig. 11b presents the joint angle trajectories of this motion. The polynomial coefficient obtained is 0.04138.

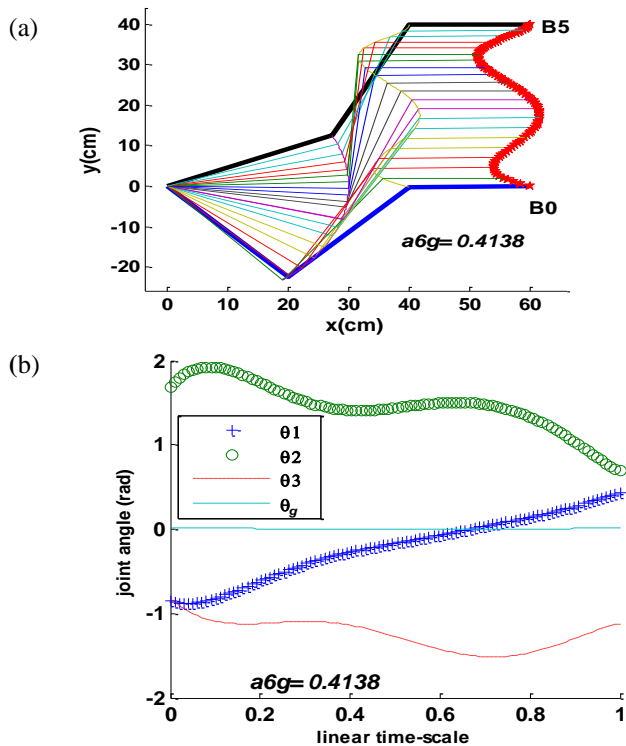


Figure 11. Case II. (a). Motion envelope (b). Joint angle trajectories

C. Error in position when s_2 solution is complex number

Next investigation is the effect of the imaginary number in (4). Case II is used to investigate the effect of the imaginary number in (4).

Figure 12 shows the motion envelope of wrong composition of initial and final configuration. In this case, the initial configuration used is $[-0.32922 \ 1.2652 \ 4.5393]$ rad while the final configuration is $[0.047179 \ 1.0335 \ -0.42988]$ rad. Figure

13 shows the detail of the end-effector position error. The joint angle trajectories of this case can be viewed in Fig. 14. It can be observed that at the position errors, the solutions of (4) contain the imaginary numbers.

Figures 15a and 15b are the motion envelope and the joint angle trajectories of the second example of wrong initial and final postures that yield the position errors. For this second example, the initial configuration is $[-0.95493 \ 1.622 \ -0.366625]$ rad and the final configuration is $[0.080225 \ 1.0365 \ 5.7272]$ rad.

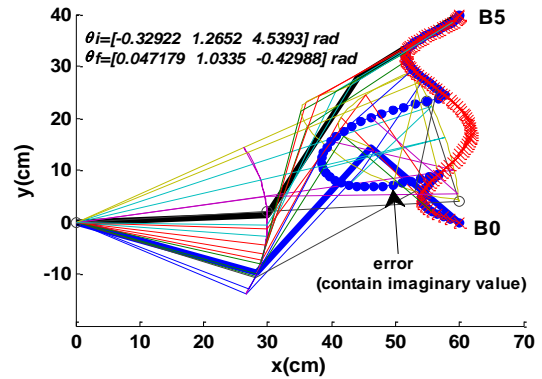


Figure 12. Position errors due to wrong composition of initial and final joint angles in case II.

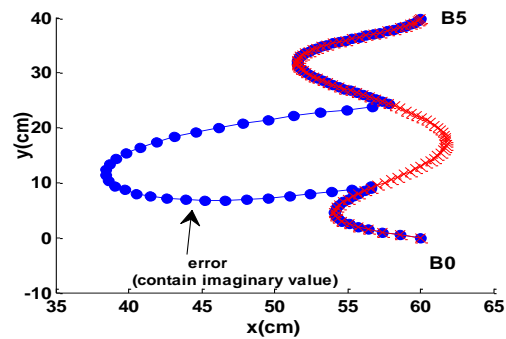


Figure 13. Detail of position errors

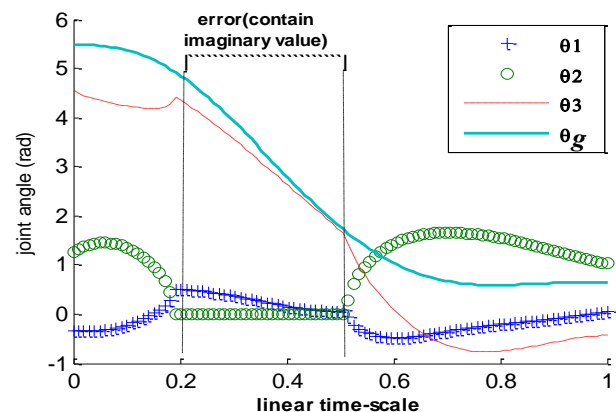


Figure 14. Imaginary values in joint angle trajectories

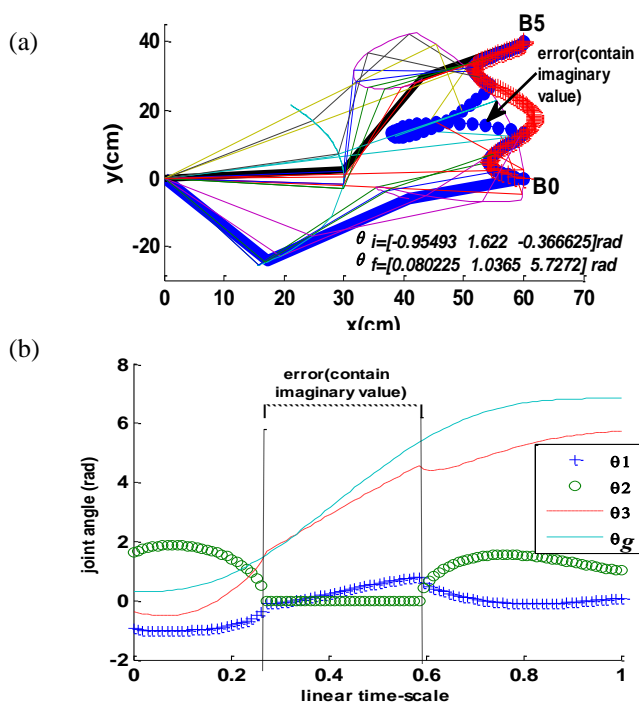


Figure 15. Another example of position errors due to wrong composition of initial and final joint angles in case II.

The self-motion behavior when the arm robot manipulator tracks the predefined path has been investigated. Modeling the joint angle in the form of polynomial function is very interesting approach because the polynomial function has many advantages. It is simple, smooth, and guarantees the continuity till $(n-1)^{\text{th}}$ derivative for polynomial function degree n . Some composition of initial and final joint angles can track the curve perfectly, but it is also possible that the composition of initial and final joint angles yields the set of the solutions of (4) contain the imaginary numbers. When these imaginary values involved, it is a sign that there are position errors at the corresponding theta global. Wrong composition of initial and final joint angle can lead the unfeasible motion where there are position errors experienced.

This result is very useful information for practical consideration. When s_2 trajectories of (4) contain complex number, there will be position errors in the part of imaginary numbers present. The position of initial and final joint angle can be reconstructed to achieve the proper composition of the initial and final joint angles. In this case, the self-motion planning needs to be executed to place the initial configuration to the correct position. Using the complex number in the motion of the robotic arm has also been investigated firstly by [19]. For the future research, there is possibility that the complex number analysis cannot be ignored in the motion planning of robotic arm. Further investigation in this issue needs to be conducted.

VI. CONCLUSION

The self-motion behaviors of 3-DOF planar series manipulator to solve the problem of the continuous path planning had been investigated. The theta global continuous function, which was developed from the 3-DOF planar robot closed form of the IK solution at one instantaneous point, had

many possible motion envelopes to track the predefined end-effector path. The GA had succeeded to solve the continuous path planning where the manipulator tracked the desired path and achieved the optimal motion. When the solutions of the theta global contained the imaginary number, the repairing of the theta global trajectories was necessary by considering the self-motion capability of the redundant manipulator. Further investigation in using the complex number in analyzing the arm robot motion was very fascinating future research to be conducted.

REFERENCES

- [1] G. Oriolo, "Stabilization of self-motions in redundant robots," in Proc. *IEEE Conference in Robotics and Automation*. California, USA, 1994.
- [2] J.W. Burdick, "On the inverse kinematics of redundant manipulators: characterization of the self-motion manifolds," in Proc. *IEEE Conference in Robotics and Automation*. Scottsdale, Arizona, 1989.
- [3] Z. Yao and K. Gupta, "Self-Motion graph in path planning for redundant robots along specified end-effector paths" in Proc. *IEEE International Conference on Robotics and Automation*. Orlando, Florida, 2006
- [4] Z. Yao and K. Gupta, "Path planning with general end-effector constraints: using task space to guide configuration space search" in Proc. *IEEE/RSJ International Conference on Intelligent Robots and Systems*. Edmonton, AB, Canada, 2005
- [5] Z. Yao and K. Gupta, "Path planning with general end-effector constraints", *Rob. Auton. Syst.* 2007, vol. 55, pp. 316–327.
- [6] C. L. Luck, "Self-Motion Representation and Global Path Planning Optimization for Redundant Manipulators through Topology-Based Discretization", *J. Intell. Robot. Syst.* 1997, vol 19, pp. 23–38.
- [7] C. L. Luck, S. Lee, "Self-Motion Topology for Redundant Manipulators with Joint Limits", in Proc. *IEEE Conference in Robotics and Automation*. USA, 1993
- [8] Y. Zhang, Y. Huang, D. Guo, "Self-Motion Planning of Functionally Redundant PUMA560 Manipulator via Quadratic-Program Formulation and Solution" In Proc *IEE International Conference on Mechatronics and Automation*. Changchun, China, 2009
- [9] Machmudah, A., Parman, S., & Baharom, M. B. (2018). Continuous path planning of kinematically redundant manipulator using particle swarm optimization. *Int. J. Adv. Comput. Sci. Appl.*, vol. 9, no. 3, pp. 207–217.
- [10] Lin, Y.; Wang, J.; Xiao, X.; Qu, J.; Qin, F. A snake-inspired path planning algorithm based on reinforcement learning and self-motion for hyper-redundant manipulators. *Int. J. Robot. Syst.* 2022, vol. 19, no.4, pp. 1–13.
- [11] M. G. Marcos, J. A. T. Machado, T-P. Azavedo-Perdicoulis, A multi-objective approach for the motion planning of redundant manipulators" *Appl. Soft Comput.* Vol. 12, no.2, pp. 589-599.
- [12] B. Karlik and S. Aydin, "An improved approach to the solution of inverse kinematics problems for robot manipulators", *Eng. Appl. Artif. Intell.* 2000, vol. 13, no.2, pp. 159-164.
- [13] J. M. Ahuactzin, K. Gupta, "A motion planning based approach for inverse kinematics of redundant robots: the kinematic roadmap", *Expert Syst. Appl.* 1998, vol 14, no. 1-2, pp. 159-167
- [14] S. Bertrand, O. Bruneau, F.B. Ouezdou, S. Alfayad, "Closed-form solutions of inverse kinematic models for the control of a biped robot with 8 active degrees of freedom per leg" *Mech. Mach. Theory* 2012, vol 49, pp. 117-140.
- [15] P. Kalra, P.B. Mahaprata, D. K. Aggarwal, "An evolutionary approach for solving the multimodal inverse kinematics problem of industrial robots", *Mech. Mach. Theory* 2006, vol. 41, no. 10, pp. 1213-1229.
- [16] S.K. Saha., *Introduction to robotics*. New Delhi, India: McGraw-Hill, 2008.
- [17] S.N. Sivanandam and S.N. Deepa, *Introduction to Genetic Algorithm*. India: Springer, 2008.
- [18] A. Machmudah, S. Parman, A. Zainuddin, and S. Chacko, Polynomial continuous joint angle arm robot motion planning in complex geometrical obstacles, *Appl. Soft Comput.* 2012, vol 13, n0. 2, pp. 1099-1109
- [19] C. W. Wampler, "Solving the kinematics of planar mechanisms," *ASME J. Mech. Des.* 1999, vol. 121, no. 3, pp. 387–391.



Setyamartana Parman graduated with a bachelor's degree in Mechanical Engineering from the Institut Teknologi Bandung and obtained a Doctor of Engineering degree from Nagaoka University of Technology in the field of Computational Mechanics. After several years working at the Indonesian Aircraft Industry IPTN he became a lecturer at the Department of Aerospace Engineering ITB. Since 2006 he has been a lecturer at Universiti Sains Malaysia, and then moved to Universiti Teknologi Petronas. He is currently a senior lecturer at Universiti Teknikal Malaysia Melaka. His interest includes computational mechanics, dynamics and control, and intelligent computing. He published more than 70 articles, both in journals and in conference proceedings.



Assoc. Prof. Dr. Ir. Mahmud Iwan Solihin is an associate professor in mechatronics engineering department (UCSI University, Malaysia) specialized in applications of artificial intelligence/machine learning, data-driven spectroscopy, meta-heuristics optimization, robotics and control systems. In the past, he was a research assistant for an eScienceFund project under MOSTI (Ministry of Science Technology & Innovation), Malaysia. He is also a professional member of the Institution of Engineers of Indonesia and recognized by AFEO (ASEAN Federation of Engineering Organisations) and APEC Engineer. He has been involved in some research projects such as from MOHE (Ministry of Higher Education), research collaborations and consultancy project on applications of machine learning, IoT and data-driven modelling in various fields including food science/agriculture, water resource management, and smart engineering systems.